# INFLUENCE OF PORCELAIN TILE STARTING COMPOSITION ON TILE MICROSTRUCTURE AND MECHANICAL PROPERTIES

### Agenor De Noni Junior<sup>(1,2)</sup>, Dachamir Hotza<sup>(2)</sup>, Vicente Cantavella Soler<sup>(3)</sup>, Enrique Sanchez Vilches<sup>(3)</sup>

 <sup>(1)</sup> Instituto Maximiliano Gaidzinski, IMG, Rua: Dr. Edson Gaidzinski, 352, CEP. 88845-000 Cocal do Sul, SC, Brazil. agenor@imgnet.org.br
<sup>(2)</sup> Universidade Federal de Santa Catarina, PGMAT/UFSC, Florianópolis, Brazil.
<sup>(3)</sup> Instituto de Tecnología Cerámica, ITC. Asociación de Investigación de las Industrias Cerámicas, AICE, Universidad Jaume I de Castellón, Spain.

#### ABSTRACT

The objective of the present study was to analyse the relation between porcelain tile starting composition and tile microstructure and mechanical properties. Seven starting mixtures were prepared for this purpose, using experimental design in the quartz-kaolin-sodium feldspar ternary diagram, varying each constituent in a range of 30% by weight (quartz: 10-40%; kaolin: 20-50%; sodium feldspar: 40-70%). It was sought to reproduce industrial processing conditions in the laboratory as faithfully as possible. The firing temperature used was the maximum densification temperature. The mechanical behaviour of the pieces was evaluated by determining their bending strength and toughness.

In regard to the starting composition, it was verified that the presence of kaolinite increased green density significantly up to kaolinite contents of 30%; at higher percentages the particles were able to interconnect with each other. The internal porosity of the sintered pieces hardly changed as a function of the composition in the studied ranges; however, the porosity of the polished product increased as the quartz content was raised, owing to quartz grain detachment during polishing.

In regard to mechanical properties, mechanical strength was found to increase as the quartz content rose. These results confirm the strengthening role that quartz particles have on the glassy matrix. On the basis of linear elastic fracture mechanics, this trend may be attributed to the variation undergone by toughness and natural flaw size. In the compositional range analysed, toughness increased when either quartz content or feldspar content rose in the starting composition. However, compositions with excessive albite content gave rise to pieces with high residual albite content, which led to a notable increase in natural flaw size and, hence, to a reduction in mechanical strength. When the kaolin content in the starting composition increased, the glassy matrix became richer in kaolinite glass, which adversely affected mechanical strength.

# 1. INTRODUCTION

Porcelain tile is a high-performance ceramic tile, basically formulated from a triaxial mixture of clay material, quartz, and feldspar. The clay material favours forming, since it contributes plasticity and dry mechanical strength, and gives rise to mullite and glassy phase formation during firing. The feldspar forms glassy phase at low temperature and encourages the sintering process, which allows attainment of practically zero apparent porosity (<0,5%) and a low level of closed porosity (3–7%). The quartz contributes to thermal and dimensional stability, since it is the constituent with the highest melting temperature.<sup>[1-5]</sup>

Industrial porcelain tile processing essentially comprises three stages: (1) preparation of the mixture by wet milling and homogenising the raw materials followed by spray drying of the resulting suspension; (2) forming by pressing the spray-dried powder with moisture content of 5-7 % at a pressing pressure of 40–50 MPa; (3) firing, in a cold-to-cold rapid cycle of 40–60 min. and peak temperature of 1180–1220 °C, defined as a function of the maximum densification obtained.

The most recent research work<sup>[6-9]</sup> notes the need to increase the knowledge of the relation existing between the starting composition, composition processing, and the microstructure of the sintered pieces, with a view to optimising porcelain tile properties. The present study has been undertaken with that aim, in regard to the mechanical properties. The compositions were developed according to the triaxial mixture (kaolin-quartz-feldspar) design method. First, porcelain tile microstructure and the phases in the fired product were characterised. The influence of porcelain tile composition on the mechanical properties of the end product was analysed, evaluated on the basis of linear elastic fracture mechanics.

# 2. BASIC THEORETICAL CONCEPTS

# 2.1. LINEAR ELASTIC FRACTURE MECHANICS

In accordance with linear elastic fracture mechanics, the mechanical strength of a material is mathematically defined by the Irwin equation, Eq. (1):

(1) 
$$\sigma_f = \frac{K_{Ic}}{Y \cdot a^{1/2}}$$

where: K  $_{\mbox{\tiny Ic}}$  , fracture toughness; a, natural flaw size; Y, fracture mechanics calibration factor.

According to this equation, the mechanical strength of a ceramic material is controlled and can be characterised by two factors: toughness and natural flaw size. In practice, mechanical strength and toughness are generally determined by independent mechanical tests, and the natural flaw size is then calculated from Eq. (1) as a fitting parameter.

# 2.2. MECHANICAL REINFORCEMENT MECHANISMS IN TRIAXIAL PORCELAINS

Although the reinforcement mechanisms in triaxial porcelains<sup>[10-14]</sup> have historically generated a certain controversy in the literature, the existence of three principal mechanisms is widely accepted: interconnection of acicular mullite crystals; dispersion of crystalline phases that limit the natural flaw size and cause the fracture to deviate; and strengthening of the matrix associated with the difference between the coefficients of linear thermal expansion of the matrix and of the dispersed crystalline phases (mainly quartz). Given the similarity with porcelains, these reinforcement mechanisms can also be applied to porcelain tile<sup>[6]</sup>.

The mineralogical and chemical composition of the product and the characteristics of the manufacturing processes determine which of these mechanisms predominates. However, they usually act simultaneously, making it difficult to establish categorically which contributes most. In addition to these factors, the negative effect of porosity on porcelain tile mechanical behaviour has also been widely documented <sup>[6,10,17-20]</sup>.

#### 3. EXPERIMENTAL PROCEDURE

#### 3.1. MATERIALS USED

To conduct the present research, high-purity raw materials were chosen with a view to avoiding the possible interaction of contaminants. Super Standard Porcelain kaolin (Imerys), quartz SE100 (Sibelco), and a floated sodium feldspar (Kaltun) were used, respectively, as a source of kaolinite, quartz, and albite. The mineralogical and chemical compositions of these raw materials are detailed in Table I. Figure 1 presents their particle size distributions. It may be observed that the kaolin has a great colloidal fraction, which allows it to contribute plasticity to the mixtures. The quartz and feldspar display practically the same particle size distribution, which resembles the distributions used in industrial practice<sup>[7]</sup>.

	Kaolin	Quartz	Feldspar
SiO <sub>2</sub>	47	98,9	68
Al <sub>2</sub> O <sub>3</sub>	38	0,51	19,2
Na <sub>2</sub> O	0,15	0,01	10,9
K <sub>2</sub> O	0,80	0,06	0,23
CaO	0,10	0,03	1,1
Others	0,64	0,11	0,34
LOI	13,0	0,27	0,14
Kaolinite	93	1	0
Albite	1	0	91
Quartz	1	98	6
Others	5	1	3

Table I. Chemical and mineralogical composition of the materials used (% weight).

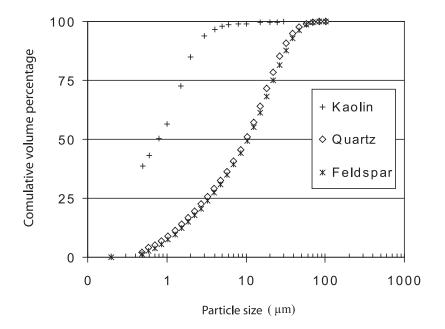


Figure 1. Particle size distribution of the materials used

# 3.2. TRIAXIAL MIXTURE DESIGN

Seven different compositions were prepared using the triaxial mixture (kaolinquartz-feldspar) design method. This method, whose usefulness has been recently verified<sup>[20]</sup>, allows systematic determination of the possible interactions between the constituents as well as the role of each constituent in the development of the properties of interest. Its principle is based on the statistical determination of constant property lines as a function of the composition within a region of interest, in which some points are experimentally measured. As a porcelain tile composition is involved, only a part of the compositions diagram can be exploited owing to the characteristics of the end product and processing constraints. The raw materials were proportioned to obtain mixtures with a major mineralogical composition in kaolinite, quartz, and albite, as indicated in Figure 2. Industrial compositions are located approximately around mixture C7, so that this composition, together with the other compositions, fully encompasses the range found in industrial practice. Figure 2 shows the experimental region studied and the location of the mixtures in relation to the entire compositions diagram. When smaller regions in the entire diagram are studied, the vertices of those regions are termed the pseudocomponents of the diagram. The vertices of the compositions with the largest quartz (C1), kaolinite (C2), and albite (C3) contents have therefore been termed pseudo-quartz (P-Quartz), pseudo-kaolinite (P-Kaolinite), and pseudo-albite (P-Albite), respectively. The triaxial diagrams have been prepared with StatSoft-STATÍSTICA version 5.5 software.

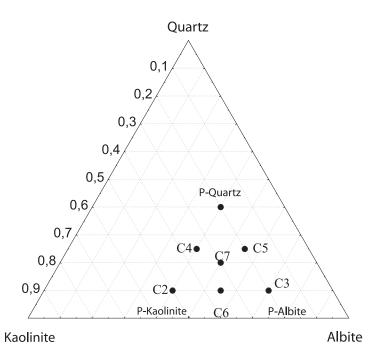


Figure 2. Experimental region and tested compositions in the triaxial mixture (quartz-kaolinite-albite). diagram

#### 3.3. PREPARATION OF THE TEST PIECES

With a view to reproducing industrial processing conditions in the laboratory as faithfully as possible, the mixtures were wet milled and homogenised for 45 min. and then spray dried. The suspensions were prepared with a solids content of approximately 65% by weight, and deflocculated with a polymer dispersant. Test pieces of 80x20x7 mm were formed by pressing at 45 MPa and 5,5% moisture content (dry basis). They were dried in an oven at 110 °C and fired in an electric kiln at a heating rate of 70 °C/min from 25 to 500 °C, and at 25 °C/min from 500 °C to peak firing temperature. The peak firing temperature used corresponded to the temperature at which maximum densification was obtained, which was determined for each mixture using the same experimental conditions as those described.

#### 3.4. TESTS CONDUCTED

Bulk density of the dry and fired test pieces was determined (Archimedes method). The real density was measured (using a helium pycnometer) in some fired test pieces of each mixture. Fired test piece cross-sections were polished to evaluate test piece porosity by optical microscopy and to examine test piece microstructure by SEM.

Bending strength was determined by three point-bending tests on ten test pieces for each mixture, using a universal mechanical testing machine (Instron 6027). Fracture toughness was determined with six test pieces by the SENB method, using a notch of about 40% of sample thickness. Natural flaw size was estimated in accordance with Eq. (1). The topography of the fracture surface of the pieces broken in the toughness test were characterised in a roughness meter (Hommelwerke, T8000) through the Sdr parameter, which represents the increase in real surface area, Ar, with respect to the projected area, Ap (1.5x1.5 mm)<sup>[21]</sup>. This Sdr parameter can be defined in accordance with Eq. 2.

(2)

$$Sdr = \frac{Ar - Ap}{Ap} \cdot 100$$

#### 4. **RESULTS AND DISCUSSION**

#### 4.1. COMPACTNESS OF THE PRESSED PIECES

Figure 3 presents the green bulk density results. Both quartz and feldspar are non-plastic constituents and have the same particle size distribution; therefore, they behave similarly with respect to packing and densification in the compaction step. Kaolinite contributes plasticity to the system, the particles are smaller, and they lodge between the particles of the non-plastic materials. Bulk density is observed to rise only when the quantity of kaolinite in the mixture increases. However, above a mass fraction of 0,30 (mixture C7), this increase is negligible. This value is consistent with the fine and coarse particle packing diagrams<sup>[22]</sup> and it indicates that the kaolinite particles already occupy practically all the spaces between the non-plastic particles, which is why they are interconnected and are unable further to increase density under these compaction conditions.

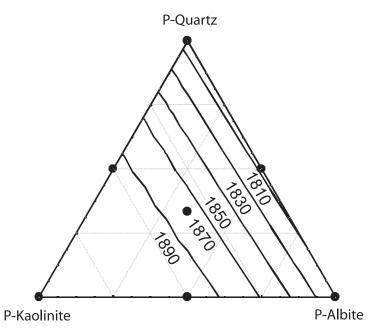


Figure 3. Green bulk density  $(kg/m^3)$  as a function of mixture composition.

#### 4.2. POROSITY OF THE FIRED PIECES

Figures 4a and 4b show, respectively, the results of total porosity calculated from the relation between real density and bulk density of the fired test pieces and from the porosity determined on the polished cross-sectional surfaces. This last porosity is of great interest, since an important part of porcelain tile production is marketed as a polished product. A decreasing trend in porosity is observed as the kaolinite content in the mixture increases. This trend is probably associated both with a larger green bulk density and with a smaller pore size distribution, which facilitate the sintering process<sup>[23]</sup>. In turn, when the quartz content is raised, porosity increases because of both the smaller green bulk density of the test pieces and the smaller content in albite in the mixture. In addition, the larger the quartz content, the greater is the difference between surface porosity and total porosity. The detachment of quartz particles during polishing is the main factor increasing surface porosity.

Since industrial compositions lie in a range of about 3,5–4,5% total porosity, once the maximum densification condition has been established, the variation in porosity is not affected very much by the composition of the product. However, for surface porosity, which is directly related to surface properties such as gloss and stain resistance<sup>[7,8]</sup>, the effect of the composition (i.e. of quartz content) is more pronounced, because for industrial compositions this lies approximately in a range of variation of 5,5–8,0%.

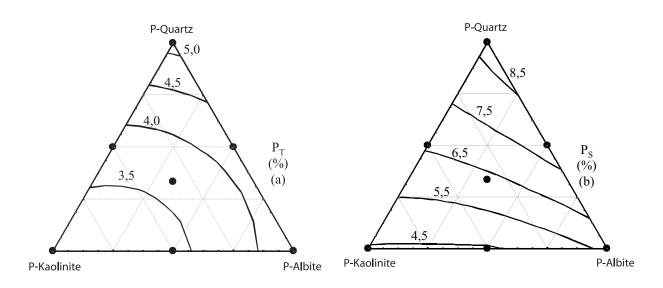
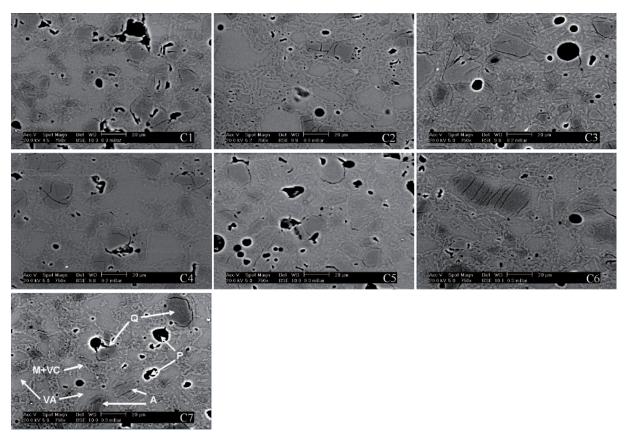


Figure 4. Total porosity,  $P_{T}$ , values (a) and surface porosity,  $P_{s}$ , values (b) as a function of the mixture composition

#### 4.3. ANALYSIS OF THE MICROSTRUCTURE OF THE SINTERED PIECES

Figure 5 presents a sequence of micrographs obtained by SEM of test pieces sintered corresponding to the seven studied compositions. All the system constituents have been marked in the micrograph of composition C7: closed porosity (P), quartz particles (Q), albite particles (A), albite glass (VA), primary mullite<sup>[24]</sup> (M), and kaolin glass (VC).

The mullite and kaolin glass share the same location, though the contrast observed is due to the mullite. These phases are located in the interfaces between the quartz particles and the glassy phase originating from the feldspar. It may be observed that for the compositions with a smaller initial kaolinite content (C1, C3, and C5), the small quantity of mullite formed does not manage to become interconnected. For the compositions with a kaolinite content above 0,30 (C7, C6, C4, C2), the mullite already exhibits that interconnection. These observations are consistent with the results of green bulk density described previously, where the effect of this particle interconnection on pressed test piece compactness was verified.



*Figure 5. Micrographs of the fired test pieces made from the studied mixtures: porosity (P), quartz (Q), albite (A), albite glass (VA), primary mullite (M), kaolin glass (VC).* 

With regard to the albite, in the compositions where residual albite remains (C3, C5, C6, and C7), the particles occupy the centre of a region rich in glassy phase resulting from their own fusion. In addition, these particles display no peripheral cracks, though they some may be broken owing to the polishing process for the sample preparation<sup>[15,17]</sup>. The appearance of the regions bounded by the glassy phase originating from the albite, characterised by the presence of mullite, preserves with great sharpness the appearance of the precursor albite particles. This observation underscores, once again, the role of kaolinite in the particle packing and densification that place takes during the forming stage.

The quartz, in turn, appears dispersed throughout the material and can be mainly identified by the presence of peripheral cracks around the particles, which may be either broken or whole. Around the quartz particles interface there is both glassy phase and mullite.

Porcelain tile microstructure is marked, therefore, by the green particle packing. The short residence time at peak firing temperature prevents the development of a significant diffusion process in the glassy phase. As a result, this phase consists principally of: (1) the matrix (VA), originating from the fusion of albite, mainly responsible for the sintering process; (2) the glass originating from kaolinite (VC), made up of silica and alumina that were not transformed into mullite. The amorphous silica, originating from the dissolution of quartz, constitutes the least significant part of the glassy phase in the porcelain tile.

#### 4.4. ANALYSIS OF THE MECHANICAL PROPERTIES OF THE TEST PIECES

Table II gives the mechanical properties characterisation data of the pieces made from the test mixtures. The experimental errors for mechanical strength and fracture toughness displayed maximum values of ~5%. The propagated error for natural flaw size was ~10%. The values of the errors were smaller than the differences between the absolute values of the properties measured. However, for natural flaw size, the errors were of the same magnitude as the variations observed, except for mixture C3. Nevertheless, a slight continuous trend may be observed, involving a decreasing natural flaw size as (M+VC) content increases; i.e. C1,C5 > C7 > C6,C4 > C2.

	σ <sub>f</sub> [MPa]	K <sub>IC</sub> [MPa·m <sup>1/2</sup> ]	a [µm]
C1	73,0 ±2,8	1,74 ±0,07	145 ±13
C2	61,7 ±3,0	1,38 ±0,09	127 ±18
C3	61,9 ±3,2	1,68 ±0,03	187 ±8
C4	70,1 ±3,1	1,59 ±0,07	131 ±11
C5	72,9 ±0,8	1,72 ±0,07	142 ±12
C6	66,7 ±2,1	1,53 ±0,07	133 ±13
C7	70,4 ±1,7	1,62 ±0,06	135 ±10

Table II. Mechanical properties (mechanical strength,  $\sigma_p$ , toughness,  $K_{IC}$ ) and natural flaw size (a) of the pieces obtained from the test mixtures

Figures 6a, 6b, 6c, and 6d present the graphs of the variation of mechanical strength,  $\sigma_f$ , toughness, K<sub>IC</sub>, natural flaw size (a), and the fracture surface tortuosity parameter (Sdr), respectively, as a function of the system constituent contents, expressed as pseudocomponents. They show clearly that the mechanical strength of the pieces increases with quartz content. In fact, the property (mechanical strength) curves follow the direction marked by the vertex bisector of the composition with the largest quartz content (composition C1) almost symmetrically, which is the composition that exhibits the highest mechanical strength. This observed trend confirms the mechanical strengthening role of the quartz in the glassy matrix of the porcelain tile. This role has been detailed, not without some controversy, in the literature. Although it was not the intention of the present research to examinee the mechanical reinforcement mechanisms, these mechanisms are basically related to the microscopic residual stress associated with the difference in thermal expansion between quartz particles ( $\alpha_0$ ) and the glassy matrix  $(\alpha_{VA})^{[25]}$   $(\alpha_O > \alpha_{VA})$ , as well as with the combination of the crack deviation and microcracking mechanisms<sup>[25]</sup>. The significant presence of cracks around the quartz particles (micrographs in Figure 5) highlights the possible contribution of these two last energy dissipating mechanisms.

The influence of the starting composition on porcelain tile mechanical strength can be analysed on the basis of linear elastic fracture mechanics (Eq. 1), which fits the fracture of this type of ceramic material<sup>[27]</sup>. Thus, Figures 6b and 6c display, respectively, the variation in regard to the starting composition of the other two parameters of the

Irwin equation, toughness and natural flaw size. Figure 6b shows that toughness increases as the kaolin content decreases or, in other words, when quartz and/or feldspar increases. In the case of quartz, some of the mechanisms responsible for the increase in toughness have already been indicated. Feldspar behaves more strikingly, because unlike for quartz it is not possible to attribute a reinforcing effect (increased toughness) owing to stresses associated with the difference in thermal expansion between the feldspar and the glassy matrix, since they are very similar (as indicated in section 3.3, the matrix consists mainly of albite glass). However, the high toughness in the feldspar vertex (composition C3) comes from the great quantity of undissolved albite particles, which cause a great deviation in the fracture propagation, as Figure 6d shows, in the highest value of the Sdr parameter (fracture surface tortuosity) corresponds precisely to this composition.

The fact that the increase in feldspar content does not raise mechanical strength, as it does with quartz, is related to the natural flaw size. Indeed, though the natural flaw size undergoes no great variation in the compositional range analysed (Table II), the vertex corresponding to the composition with the largest feldspar content (composition C3) has given rise to pieces with an exceptionally large flaw, which would explain the fact that the mechanical strength of the compositions close to this vertex was smaller than might be expected, based on their toughness values. A possible explanation would again be the presence of a large quantity of unmelted albite particles, clearly evidenced in the micrograph of composition C3 in Figure 5.

On the other hand, in regard to the influence of kaolinite (kaolin) on mechanical properties, the results show that as the kaolin content in the starting mixture increases, the mechanical strength of the pieces decreases, as a result of the reduced toughness. This outcome is especially noteworthy, because despite the reduction in porosity (Figure 4a) and even of natural flaw size with the increased kaolin content (Figure 6c), the weakening of the matrix is so pronounced that it counteracts these effects. Thus, an increase in kaolin content will give rise to greater mullite crystallisation but particularly, given the system's thermodynamic non-equilibrium condition owing the high firing rate, to a greater quantity of kaolinite amorphous phase (glass) (see micrograph of composition C2 in Figure 5), which clearly worsens matrix resistance to crack propagation. This last point is corroborated when the evolution of fracture tortuosity is observed (Figure 6d), because as the kaolin content increases, the Sdr parameter becomes appreciably smaller.

Finally, the mechanical strengthening role of mullite crystals apparently fails to develop, basically for two reasons: (1) their small crystal size, since they stem from the thermal decomposition of kaolinite particles ( $85\% < 2 \mu m$ ), which mainly gives rise to granular crystals of primary mullite, with hardly any dissolution and subsequent devitrification (these characteristics of the crystallised mullite can also be observed in the micrographs of Figure 5); (2) the coefficient of thermal expansion of the crystals of both the primary mullite and the kaolin glass is smaller than that of the glassy matrix, which produces a counter effect to that of the quartz particles, i.e. weakening of the matrix.

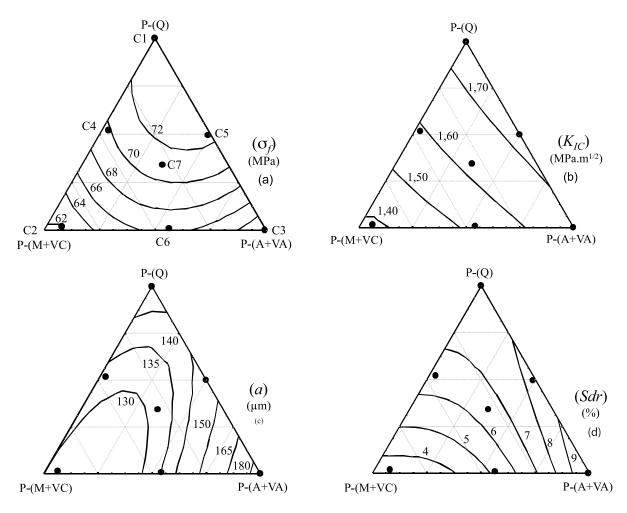


Figure 6. a) Bending strength ( $\sigma_f$ ), b) toughness ( $K_{IC}$ ), c) natural flaw size and d) tortuosity of the porcelain tile fracture surface as a function of system constituent contents.

# 5. CONCLUSIONS

Microstructural and mechanical characterisation was performed of the fired pieces obtained from porcelain tile compositions formulated using the triaxial mixture design method. The study allows the following conclusions to be drawn:

Kaolinite contributes plasticity to the mixture and favours the increase in green bulk density of the pressed test pieces. However, when the quantity of kaolinite particles is sufficient for them to become interconnected, successive additions do not increase compactness, but may even decrease it.

Considering the maximum density condition as a criterion for the obtainment of the porcelain tile, total porosity does not change too much with regard to the starting composition. However, surface porosity does increase appreciably after the polishing process, when the quartz content is raised in the starting mixture, owing to quartz grain detachment during polishing. The mechanical strength of the pieces increases clearly when the quartz content increases. This trend is marked by the evolution that toughness undergoes with the increase in quartz content and confirms the mechanical strengthening role of the dispersed quartz particles in the glassy matrix. However, although toughness also increases when the feldspar content is raised in the initial composition, when the initial albite content is very large (70%), natural flaw size also rises owing to the dispersed albite crystals that do not fuse completely. Both parameters (toughness and flaw size) cancel each other out, which is why the effect of feldspar on mechanical strength is of little note.

Finally, it was verified that when the mullite and kaolinite glass content in the sintered pieces increased, obtained by using kaolin-rich starting compositions, toughness worsened significantly, and with it the material's mechanical strength, which invalidates the hypothesis that mullite acts as a reinforcement mechanism in porcelain tile, unlike what occurs in porcelains. This might be related to the weakening of the glassy matrix, since these constituents (primary mullite + kaolin glass) have a smaller coefficient of thermal expansion than the glass originating from albite.

#### 6. ACKNOWLEDGEMENTS

The authors thank the staff of the Instituto de Tecnología Cerámica – ITC, Spain. They also thank the "Coordenação de Aperfeiçoamento de Pessoal de Nível Superior" – CAPES, Brazil, and the Instituto Maximiliano Gaidzinski – IMG, Brazil. Finally, they express their gratitude to the Spanish Ministry of Industry, Tourism and Commerce for the co-financing given in the Horizontal Programme in support of technology centres (FIT-030000-2005-315/FIT-030000-2006-119).

#### REFERENCES

- [1] Manfredini, T. Pellacani, G.C. & Romagnoli, M. Porcelainized stoneware tile. Am. Ceram. Soc. Bull., 1995, 74, 76-79.
- [2] Sánchez, E. Orts, M.J. Ten, J.G. & Cantavella, V., Porcelain tile composition: effect on phase formation and end products. Am. Ceram. Soc. Bull., 2001, 80, 43-49.
- [3] Leonelli, C. Bondioli, F. Veronesi, P. Romagnoli, M. Manfredini, T. Pellacani, G.C. Cannillo, V. Enhancing the mechanical properties of porcelain stoneware tiles: a microstructural approach. J. Eur. Ceram. Soc, 2001, 21, 785-793.
- [4] Biffi, G., Il gres porcellanato: manuale di frabricacione e tecniche di impego. Faenza editrice, Faenza, 1997.
- [5] Norton, F.H. Elements of ceramics. Ed. Addison-Wesley, Ed. Addison Wesley, Massachussets UK, 1975.
- [6] Cavalcante, P.M.T, Dondi, M. Ercolani, G. Guarini, G. Melandri, C. Raimondo, M. Almendra, E.R. The Influence of Microstructure on the Performace of White Porcelain Stoneware. Ceram. Int., 2004, 30, 953-963.
- [7] Hutchings, I.M. Xu, Y. Sánchez, E. Ibáñez, M.J. Quereda, M.F. Porcelain tile microstructure: Implications for polishability. J. Eur. Ceram. Soc., 2006, 26, 1035-1042.
- [8] Sánchez, E. Ibáñez, M.J. García-Ten, J. Quereda, M.F. Hutchings, I.M. Xu, Y.M., Porcelain tile microstructure: implication for polished tile properties. J. Eur. Ceram. Soc., v.26, n.13, p.2533-2540, 2006.
- [9] Tucci, A. Esposito, L. Malmusi, L. Rambaldi, E. New body mixes for porcelain stoneware tiles with improved mechanical characteristics. J. Eur. Ceram. Soc., v.27, n.23, p. 1875-1881, 2007.
- [10] Stathis, G.; Ekonomakou, A.; Stournaras, C.J.; Ftikos, C. Effect of Firing Conditions, Filler Grain Size and Quartz Content on Bending Strength and Physical Properties of Sanitaryware Porcelain. Journal of the European Ceramic Society, v. 24, p. 2357-2366, 2004.

- [11] Bragança, S.R.; Bergmann, C.P.; Hübner, H. Effect of Quartz Particle Size on the Strength of Triaxial Porcelain. Journal of the European Ceramic Society, v. 26, p. 3761-3768, 2006.
- [12] Hamano, K.; Wu, Y.H.; Nakagawa, Z.; Hasegawa, M. Effect of Coarse Quartz Grain on Mechanical Strength of Porcelain Body. Journal of the Ceramic Society of Japan – International Edition, v. 99, p. 1070-1073, 1991.
- [13] Hamano, K.; Wu, Y.H.; Nakagawa, Z.; Hasegawa, M. Effect of Grain Size of Quartz on Mechanical Strength of Porcelain Bodies. Journal of the Ceramic Society of Japan – International Edition, v. 99, p. 149-153, 1991.
- [14] Warshaw, S.I.; Seider, R.J., Comparison of Strength of Triaxial Porcelains Containing Alumina and Silica. Journal of the American Ceramic Society, v. 50, p. 337-342. 1967
- [15] De Noni Jr. A. Hotza, D. Cantavella, V. Sánchez, E., Estudo das propriedades mecânicas de porcelanato através da avaliação de tensões residuais microscópicas e macroscópicas originadas durante a etapa de resfriamento do ciclo de queima. PhD thesis, Universidade Federal de Santa Catarina, Florianópolis, SC, Brazil, 2007.
- [16] Navarro, J.M.F. El Vidrio Constitución, Fabricación y Propiedades. 3<sup>rd</sup> ed.. CSIC, Madrid, Spain, 2003.
- [17] Carty, W.M.; Senapati, U. Porcelain Raw Materials, Processing, Phase Evolution, and Mechanical Behavior. Journal of the American Ceramic Society, v. 81, n. 1, p. 3-20, 1998.
- [18] Kato, E.; Satoh, T.; Ohira, O.; Kobayashi, Y. Effect of Quartz on the Sintering and Bending Strength of the Porcelain Bodies in Quartz-Feldspar-Kaolin System, Journal of the Ceramic Society of Japan – International Edition, v. 102, n.1, p.99-104, 1994.
- [19] Kobayashi, Y.; Ohira, O.; Ohashi, Y.; Kato, E. Effect of Firing Temperature on Bending Strength of Porcelain for Tableware. Journal of the American Ceramic Society, v. 75, n. 7, p. 1801-1806, 1992.
- [20] Correia, S.L.; Oliveira, A.P.N.; Hotza, D.; Segadães, A.M. Properties of Triaxial Porcelain Bodies: Interpretation of Statistical Modeling. Journal of the American Ceramic Society, v. 89, n. 11, p. 3356-3365, 2006.
- [21] Blunt, L.; Jiang, X. Advanced Techniques for Assessment Surface Topography. Kogan, London, 2003.
- [22] Oliveira, I.R.; Studart, A.R.; Pileggi, R.G.; Pandofelli, V.C. Dispersão e Empacotamento de Partículas: Princípios e Aplicações em Processamento Cerâmico. Fazendo Arte, São Paulo, 2000.
- [23] Amorós, J.L. Orts, M.J. García-Tem, J. Gozalbo, A. Sánchez, E. Effect of Green Porous Texture on Porcelain Tile Properties. Journal of European Ceramic Society, doi:10.1016/j.eur.ceramsoc.2006.07.005, 2006.
- [24] Lee. W.E. Souza, G.P. McConville, C.J. Tarvornpanich, T. Iqbal, Y. Mullite Formation in Clays and Clay-Derived Vitreous Ceramics. Journal of the European Ceramic Society, doi:10.1016/j.jeurceramsoc.2007.03.009, 2007.
- [25] Evans, A.G. Perspective on the Development of High-toughness Ceramics, Journal of the American Ceramic Society, v. 73, p. 187-206, 1990.
- [26] Vergano, P.J.; Hill, D.C.; Uhlmann D.R. Thermal Expansion of Feldspar Glasses, Journal of the American Ceramic Society, v. 50, p. 59-60, 1967
- [27] Green. D.J. Introduction to Mechanical Properties of Ceramics. Cambridge University Press, Cambridge, 1998.